Frequency selection and transient dynamics in single-mode lasers with optical feedback

E. Hernández-García
Departament de Física, Universitat de les Illes Balears, E-07071 Palma de Mallorca, Spain

N. B. Abraham
Department of Physics, Bryn Mawr College, Bryn Mawr, Pennsylvania 19010-2899

M. San Miguel and F. De Pasquale[a)]
Department de Física, Universitat de les Illes Balears, E-07071 Palma de Mallorca, Spain

(Received 26 August 1991; accepted for publication 30 April 1992)

It is demonstrated that a closed delayed equation for the phase of the electric field can be used to describe accurately the transient switch on of a laser with external feedback when it can be described by field evolution equations. In contrast, it is shown that several more severe approximations to the dynamics, including an adiabatically evolving potential for one-dimensional relaxation dynamics (which had previously been used to accurately predict the laser linewidths for the steady-state solutions) fail to reliably describe the final state selection during transient switch on of the laser, the delay-induced oscillatory approach to the chosen state, and features of the amplitude and frequency spectra near multiples of the external cavity mode spacing which may be important for the stability and switching dynamics of the steady states that correspond to excitation of different external cavity resonances.

I. INTRODUCTION

It is well known that the linewidth of a single-mode laser can be considerably narrowed by a small amount of feedback from an external mirror or resonator. If the feedback is large enough the laser can operate in several different states which have optical frequencies that are shifted with respect to the emission frequency of the laser in the absence of external feedback. For relatively small external delay times the different operating frequencies represent long-lived locally stable lasing states of the three-mirror laser that approximately correspond to selection of different ones of the resonant frequencies of the external resonator. The most stable state is the one of smallest linewidth and not the one of highest output power.[1–3] These are rather general properties of any type of laser with optical feedback and they have been considered in particular detail for single-mode laser diodes.[4,5] For cw operation, the competition among the states with different frequencies seems to be well described by a potential picture[6,7] of general applicability for different types of lasers. In this model, the difference in phase at times separated by the feedback delay time obeys a relaxational dynamics driven by noise in a potential with multiple minima. (From the simplifications of this model the dynamics of the laser frequency is determined by the evolution of the other dynamical variables of the laser, but there is no dependence of those variables on the changes in the optical frequency.) The locations of the minima of the potential are associated with the solutions of different frequency and the curvature of the potential at these minima is inversely proportional to the linewidth. The long-time hopping dynamics between the solutions having different frequencies also seems to be rather well reproduced by this model.

In this paper we address questions complementary to this description which are associated with the transient dynamics when the laser is turned on. Since the different steady-state solutions with different frequencies are in general long lived, a crucial question is which frequency is selected in each switch-on event. We are interested in the description of such frequency selection dynamics and in the characterization of the fluctuations during this dynamical regime. One of our motivations is to explore to what extent the potential picture mentioned above can describe this dynamical regime. We are not aware of any other systematic study of stochastic transient dynamics in the presence of optical feedback. The exception is the experimental work in Ref. 8 where the emission frequency is observed to change during the transient regime from a frequency close to the emission frequency in the absence of feedback to a new final frequency. Such studies of transient dynamics are of relevance for the use of these devices in coherent optical communications. They are also desirable in view of recent results[9] which indicate a possible confusion between long transients and chaoticlike solutions.

Our discussion in this paper is based on a model for the complex electric-field amplitude, appropriate for detuned single-mode lasers with high Q factor, so that the material dynamics can be adiabatically eliminated, and small to moderate feedback from a single external mirror. We neglect the possible excitation of other longitudinal modes of the free-running laser that can be effectively suppressed for many lasers by the choice of a mode spacing larger than the gain linewidth, by operation close to the lasing threshold, or by an intracavity étalon. Our results are then directly applicable to almost any laser near threshold and more generally to single-mode dye lasers and single-mode

[a)]Permanent address: Dipartamento di Fisica, Universita di l'Aquila, L'Aquila I-67100, Italy.

 0021-8979/92/161225-12$04.00

helium-neon lasers and show the interplay between transient dynamics and oscillations due to the optical feedback. The applicability of our results to other lasers such as solid-state or semiconductor lasers would require further elaboration since their proper modeling requires equations for the field and the material variables in order to describe the effects of relaxation oscillations. However, it is often found that many basic phenomena of linewidth narrowing in these more complicated lasers can be described accurately by equations for the complex field amplitude.[10] In fact a common description of frequency properties associated with optical feedback is given in terms of a Van der Pol equation.[11] Results of such models are appropriate for the external cavity geometry that is commonly used for linewidth reduction and frequency stabilization in semiconductor lasers so long as the time scales of evolution are long compared to the characteristic times for response of the carrier number. There is also a long history of analysis of this kind of model in order to gain insight into the behavior of lasers with external reflectors. In addition, it provides the simplest basis for extending the investigation of the potential picture of the phase difference to the regimes of transient and stochastic dynamics.

Our analysis is based on analytic approximations and numerical simulations of stochastic equations. We consider transients following an abrupt switch on of the gain from an initial level below the threshold for laser action. We find that the transient dynamics is characterized by a rapid frequency shift associated with the initial increase in the intensity followed by an oscillatory approach to the final state. These oscillations are associated with the feedback and should be present in any type of laser with optical feedback. While they are qualitatively similar to relaxation oscillations, the oscillations in the case have a fundamentally different origin. (It is worth noting that previous studies that include the carrier dynamics have shown that semiconductor lasers can be more susceptible to undamped pulsations when the feedback-induced oscillations match the relaxation oscillation frequency.) Although our models for the evolution of the field do not have the relaxation oscillation resonance phenomena, we can still see the degree to which the further potential-based approximations neglect features of the noise spectrum that are induced purely by the feedback, namely, line narrowing at the expense of excess power at higher frequencies.

Strong fluctuations of the frequency occur at the time of the frequency jump, but the laser approaches the state with the frequency associated with narrowest linewidth (which is not the one with highest output power) with very high probability during the transient regime. A generalization of the potential dynamics of Refs. 6 and 7 to the transient regime is seen to lead in some cases to an incorrect prediction of the frequency selected at the end of the transient and this approach cannot describe the oscillatory approach to steady state; however, it is useful for identifying the time at which the frequency jump occurs. We also introduce an approximation leading to a closed delayed equation for the phase which gives a good description of the dynamics for all times, including the oscillatory approach to the final steady state. Finally, in order to explore the spectral linewidth and stability of the solutions, we consider the effect on the steady-state spectra of the oscillations purely associated with the feedback which give rise to sidebands in the spectra. We calculate the steady-state spectra of the intensity, frequency, and the electric-field amplitude from the full equations and from the approximations considered above. Errors occur for the frequency and amplitude spectra in the potential picture near frequencies that are multiples of the spacing between external cavity modes. The power in this portion of the spectrum can be relatively large when the noise is strong. In addition, since these are important frequencies during noise-induced transitions to other states at all noise strengths, it is likely that the stability of the steady states is overestimated by the potential picture. However, the calculation of the field spectrum in terms of amplitude and frequency fluctuations indicates that the low-frequency linewidth associated with a central Lorentzian peak is accurately reproduced in any of the approximations considered here.

The importance of these results is that they clarify the effects of feedback on the temporal and spectral behavior. The feedback with delay causes oscillatory behavior which can be viewed either in the time domain or in the frequency domain, where it may be referred to as transient excitation of external cavity modes. We see in our results a distinction between temporal oscillation (AM and FM modulation) and extended or alternate operation at one or more of the external cavity modes. A potential picture provides the many different external cavity mode steady states, but it provides no mechanism for significant amounts of transient oscillations. Experimental measurements could be made to establish that oscillations do occur, ruling out the potential picture. Studies of those oscillations in time and in spectra could reveal whether they correspond to actual mode competition (as is often argued) or to phase and amplitude modulation of a single field. Additional features that arise from relaxation oscillations when they are present could also be more clearly identified. However, of most importance is the demonstration that relaxation oscillation phenomena are not essential for the appearance of an oscillatory approach to steady-state operation. While they may be resonant enhancement of the oscillatory behavior when the relaxation oscillation frequency matches the oscillations caused by feedback, there are two distinct mechanisms.

The outline of the paper is as follows. In Sec. II we introduce our dynamical model, we derive from it a potential picture, and we review some of its features and limitations. We also discuss possible approximations to describe the stochastic transient dynamics of frequency selection. In Sec. III we analyze individual switch-on events. Statistical properties of fluctuations averaged over many switch-on events are discussed in Sec. IV. In Sec. V we consider the calculation of steady-state spectra in the context of our previous results. Section VI gives a summary of our main results and conclusions.

II. APPROXIMATIONS FOR THE TRANSIENT DYNAMICS

Our starting dynamical model is the following equation for the slowly varying amplitude of the electric field $E(t)$ of a single-mode high-Q-factor laser with weak feedback from a single external mirror. It can be derived from the Lang–Kobayashi equations[12] for semiconductor lasers through the adiabatic elimination of the material variables, or it can be gotten from the single-mode equations for any detuned laser by a similar adiabatic elimination. The Lang–Kobayashi equations have been used as the starting point in Refs. 1, 3, 4, and 7, among others, for the discussion of lasers (including semiconductor lasers) with external feedback, and they have been specifically reduced to an equation of the following form in the discussions of dynamics in a potential well in Refs. 6 and 7:

$$\dot{E}(t)=(1+i\theta)[aE(t)-b|E(t)|^2E(t)]+\gamma E(t-\tau) +i\omega_0 E(t)+\sqrt{\epsilon}\xi(t). \tag{1}$$

The parameter a is the total gain parameter and b is the saturation parameter in a third-order Lamb approximation. The frequency ω_0 is the frequency of the laser when it is above threshold in the absence of feedback. The detuning parameter θ plays the role of the α factor in semiconductor lasers. The feedback coupling parameter γ is proportional to the strength of the feedback, and τ is the feedback delay time. We assume that the field is uniform inside the laser medium and that the internal round-trip time is negligibly short compared with the feedback delay time τ. Spontaneous emission noise is modeled by the complex Gaussian white noise $\xi(t)$ with intensity ϵ and correlation

$$\langle\xi(t)\xi^*(t')\rangle=4\delta(t-t'). \tag{2}$$

In terms of amplitude and phase in a rotating frame, $E(t)=A(t)e^{i[\varphi(t)+\omega_0 t]}$, Eq. (1) can be written as

$$\dot{A}(t)=aA(t)-bA(t)^3+\gamma A(t-\tau)\cos[\Delta\varphi(t)] +\sqrt{\epsilon}\xi_A(t) \tag{3}$$

and

$$\dot{\varphi}(t)=\theta[a-bA(t)^2]-\gamma\frac{A(t-\tau)}{A(t)}\sin[\Delta\varphi(t)] +\frac{\sqrt{\epsilon}}{A(t)}\xi_\varphi(t), \tag{4}$$

where

$$\Delta\varphi(t)\equiv\varphi(t)-\varphi(t-\tau)+\omega_0\tau. \tag{5}$$

The amplitude and phase noises have correlations given by

$$\langle\xi_A(t)\xi_A(t')\rangle=\langle\xi_\varphi(t)\xi_\varphi(t')\rangle=2\delta(t-t'), \tag{6}$$

and vanishing cross correlations. The steady solutions of Eqs. (3) and (4) with constant amplitude and frequency $\dot{\varphi}=\omega$ are given by

$$A^2=(a/b)+(\gamma/b)\cos[(\omega_0+\omega)\tau] \tag{7}$$

and

$$\omega\tau=-\gamma\tau\sqrt{1+\theta^2}\sin[(\omega_0+\omega)\tau+\arctan\theta]. \tag{8}$$

A necessary condition for the existence of multiple solutions of Eq. (8) is that the dressed feedback parameter $C\equiv\gamma\tau\sqrt{1+\theta^2}$ be such that $C>1$. When such solutions exist the phenomenon of frequency multistability appears.

Chaotic behavior in semiconductor lasers (including some described by this model) with feedback has been discussed by a number of authors.[3,13] The solution of Eq. (1), for $a\sim\gamma$, follows a route to chaotic behavior as τ is increased; from a monotonic relaxation, damped oscillations, periodic behavior, and eventually erratic dynamics are obtained. For a fixed value of τ this route is also followed as the ratio γ/a is increased. However, as we are primarily interested in the fluctuations during the transients and the spectra of the steady states, we will not discuss further the regimes of chaotic operation.

Throughout this paper we choose time units in which $\tau=1$. In these units we take $b=20$, $\theta=5$, and $\epsilon=10^{-20}$. We will consider two different representative parameter sets:

Set I: $\gamma=2$, $a=20$, $\omega_0=\pi$,

Set II: $\gamma=0.5$, $a=2$, $\omega_0=0$.

For these two sets, $C=10.2$ and 2.55, respectively, and the dynamics shows no chaotic behavior. Qualitatively these two sets belong to regions II/III of the classification of Ref. 14 (see also Ref. 5, page 273) for distributed feedback (DFB) lasers. Hence these two sets belong to the domain for which the potential approximation of Refs. 6 and 7 is intended to be valid. Frequency multistability only occurs for the first set of parameters.

A description of the frequency dynamics implied by Eqs. (3) and (4) in terms of a potential[6,7] requires two steps. The first step involves the assumption of a late regime in which the dynamics of the amplitude follows the phase dynamics adiabatically so that we set

$$\dot{A}\sim 0, \quad A(t-\tau)\sim A(t)$$

in Eq. (3) obtaining

$$A^2=(a/b)+(\gamma/b)\cos\Delta\varphi+(\sqrt{\epsilon}/bA)\xi_A(t). \tag{9}$$

Replacing Eq. (9) in Eq. (4), that equation for the phase becomes

$$\dot{\varphi}=-\gamma\sqrt{1+\theta^2}\sin[\Delta\varphi(t)+\arctan\theta]+q(t), \tag{10}$$

where

$$q(t)\equiv(\sqrt{\epsilon}/A)(\xi_\varphi-\theta\xi_A) \tag{11}$$

is a real Gaussian white noise with correlation

$$\langle q(t)q(t')\rangle=\frac{2\epsilon(1+\theta^2)}{A^2}\delta(t-t'). \tag{12}$$

Equation (10) describes the late time regime phase evolution with fluctuations around one of the possible final states. The value of A used in the denominator of Eq. (12) is given by Eq. (7). In this time regime A is assumed to be constant and determined from Eq. (7) by one of the

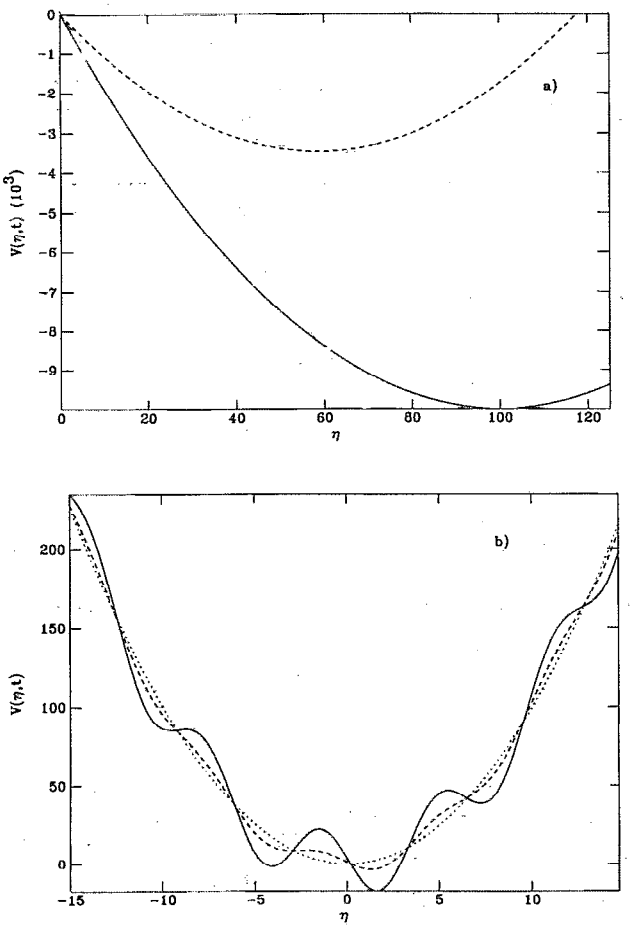

FIG. 1. The time-dependent potential $V(\eta,t)$ for set I of parameters. A value of $|h(\infty)|=\sqrt{(2\epsilon/a)}$ has been used to obtain a typical evolution. (a) Solid line: $t=1$ (indistinguishable from any $t<1$), dashed line: $t=1.20$; (b) dotted line: $t=1.40$, dashed line: $t=2.15$, solid line: $t=2.30$ [indistinguishable from $V(\eta,t=\infty)$].

steady-state solutions of Eq. (8). The second step involves the approximation of Mørk and co-workers[6] to convert this delayed equation (formally an infinite-order differential equation) into a local-in-time, first-order differential equation for the phase difference

$$\eta(t)\equiv\varphi(t)-\varphi(t-\tau). \tag{13}$$

Setting

$$\dot{\eta}\sim-(2/\tau)\eta+2\dot{\varphi}, \tag{14}$$

one obtains

$$\dot{\eta}=-\tau^{-1}\frac{\partial V(\eta)}{\partial\eta}+2q(t), \tag{15}$$

where the potential $V(\eta)$ is given by

$$V(\eta)=\eta^2-2\gamma\tau\sqrt{1+\theta^2}\cos(\eta+\omega_0\tau+\arctan\theta). \tag{16}$$

The dynamics of the variable η gives a good account of the frequency dynamics in the system for small τ. The form of this potential for our two sets of parameters is shown in Figs. 1 and 2. Each local minimum for set I of the parameters is associated with a solution of a different frequency as given by Eq. (8).

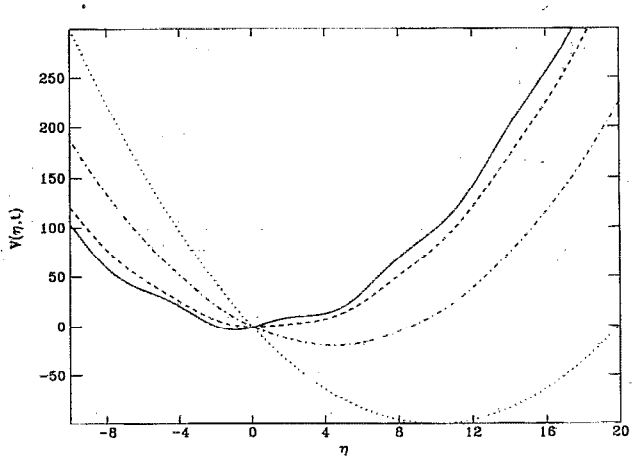

FIG. 2. Same as Fig. 1 but for set II of parameters. Dotted line: $t=9.5$, indistinguishable from any $t<9.5$, dot-dashed line: $t=11$; dashed line: $t=11.5$; solid line: $t=13$, indistinguishable from $V(\eta,t=\infty)$.

While Eq. (15) seems to give a reasonable description of steady-state properties and dynamics on long time scales,[6,7] we are interested in the transient dynamics after the laser switched on. During this transient, one of the solutions is selected. Hopping among the solutions of different frequencies occurs at much longer times. It is clear that Eq. (15) cannot describe the transient dynamics since it is based on a late time approximation for the amplitude. We now explore whether some modification of this potential picture can be successfully applied in the regime of transient dynamics. Our general strategy is to find a time-dependent approximation for the amplitude which can be then substituted into Eq. (4), to give a closed equation for the phase dynamics. A second step involving the approximation Eq. (14) should lead to a description in terms of a time-dependent potential.

In the absence of feedback ($\gamma=0$) there exists a well-known approximation for the transient dynamics of the amplitude,[15,16]

$$A_0(t)=\frac{|h(t)|}{\{e^{-2at}[1-(b/a)|h(t)|^2]+(b/a)|h(t)|^2\}^{1/2}}, \tag{17}$$

where

$$h(t)=\sqrt{\epsilon}\int_0^t e^{-at'}\xi(t')dt'. \tag{18}$$

Equation (17) can be understood as given by the deterministic solution of Eq. (3) (for $\gamma=0$) with the initial condition $A_0(0)$ replaced by $|h(t)|$. This approximation implies an amplification of an effective random initial condition $h(t)$ by the deterministic solution. For $t>1/a$, $h(t)$ can be safely replaced by $h(\infty)$ which is a complex Gaussian random number of zero average, random phase, and $\langle|h(\infty)|^2\rangle=2\epsilon/a$. The effect of feedback cannot be introduced by a straightforward perturbation in γ of the solution of Eq. (3) around Eq. (17) because of the appearance

of secular terms. An ansatz for $A(t)$ can be obtained as a generalization of Eq. (9) for all times: The adiabatic following (for $\epsilon=0$) of Eq. (9) is formally obtained setting $\dot{A}=0$ in Eq. (3),

$$A^2=\frac{a}{b}\left(1+\frac{\gamma}{\alpha}\frac{A(t-\tau)}{A(t)}\cos\Delta\varphi\right). \tag{19}$$

Noting that $A_0^2(\infty)=(a/b)$, $A^2(t)$ can be approximated during the transient regime by replacing in the right-hand side of Eq. (19) $A_0(\infty)$ and $A(t)$ by $A_0(t)$,

$$A^2(t)=A_0^2(t)\left(1+\frac{\gamma A_0(t-\tau)}{aA_0(t)}\cos\Delta\varphi\right). \tag{20}$$

$A^2(t)$ is then given by a standard approximation for $\gamma=0$ modified by a nonperturbative correction. The long time dynamics is well described since Eq. (20) reproduces Eq. (9) (for $\epsilon=0$) in this limit. For very early times the dynamics is essentially linear. Equation (20) reproduces the linear solution of Eq. (1) to lowest order (p^0) in the parameter $p\equiv\gamma e^{-a}$, so that it becomes better as p becomes smaller. For intermediate times Eq. (20) is expected to give a good interpolation between these two limits. Substituting Eq. (20) in Eq. (4) we obtain a proper generalization of Eq. (10) for transient dynamics,

$$\dot{\varphi}=\theta a\left[1-\frac{b}{a}A_0^2(t)\left(1+\frac{\gamma A_0(t-\tau)}{aA_0(t)}\cos\Delta\varphi\right)\right]$$
$$-\frac{\gamma A_0(t-\tau)}{A_0(t)}\sin\Delta\varphi+\frac{\sqrt{\epsilon}}{A_0(t)}\xi_\varphi(t). \tag{21}$$

It turns out that Eq. (21) gives correctly the terms of order p^0 and p^1 in the expansion of the exact linear solution of Eq. (1). Since it also reproduces the deterministic correct steady-state results, it is expected that for intermediate times Eq. (21) gives a good interpolation between early and late time evolution. In fact, it is shown below that it gives a very good description of the phase evolution for all times. An additional comment on noise effects is needed. The dominant noise effect during the transient dynamics is the shifting in time of the amplitude evolution due to the random switch-on times. This effect is well described in Eqs. (20) and (21) through the randomness of $A_0(t)$. However, the amplitude noise term $\xi_A(t)$ consider in Eqs. (9) and (11) is not included in Eqs. (19) and (21). The reason is that explicit amplitude noise is important in the late time regime when the system is near a steady-state solution (see Sec. V) but should not be included in the transient dynamics: Amplitude fluctuations are irrelevant in the transient dynamics after the amplitude turn on, and they cannot be included in Eq. (19) in the very early noise-dominated regime ($t<1/2a$) since it would imply an unphysical adiabatic following of white noise by the amplitude.

If the further approximation using Eq. (14) is made in Eq. (21) we obtain the generalization of Eq. (15) in which the potential V in Eq. (16) is replaced by the time-dependent potential

$$V(\eta,t)=\eta^2-2\theta a\tau[1-g(t)]\eta$$

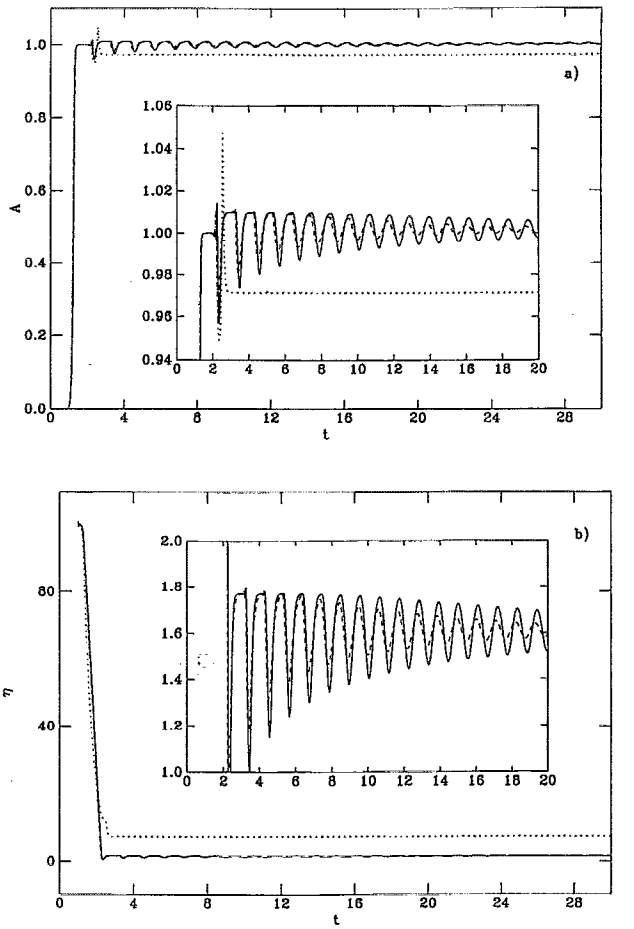

FIG. 3. (a) Amplitude and (b) η evolution for set I of parameters. Solid line: direct simulation of Eq. (1); dashed line: approximation in Eqs. (20) and (21); dotted line: time-dependent potential approximation, Eqs. (15) and (22). Note that η is not defined for $t<1$.

$$-2\gamma\tau\frac{A_0(t-\tau)}{A_0(t)}[1+\theta^2g^2(t)]^{1/2}$$
$$\times\cos\{\eta+\omega_0\tau+\arctan[\theta g(t)]\}, \tag{22}$$

where

$$g(t)\equiv bA_0^2(t)/a. \tag{23}$$

The time dependence of this potential for the two sets of parameters we are considering is also shown in Figs. 1 and 2. For $t=\infty$, $V(\eta,t=\infty)$ reproduces the potential Eq. (16). The development in time of the local minima associated with the multiple solutions of Eq. (17) (parameter set I), or the dynamic evolution of a preferred frequency (parameter set II), is clearly displayed.

III. ANALYSIS OF INDIVIDUAL SWITCH-ON EVENTS

The time evolution of the amplitude and η variables are shown in Figs. 3 and 4 as obtained from a numerical simulation of Eq. (1) and compared with simulations of the approximations Eqs. (20) and (21) and Eqs. (15) and (22). They are representative switch-on events obtained for a given sequence of random numbers associated with

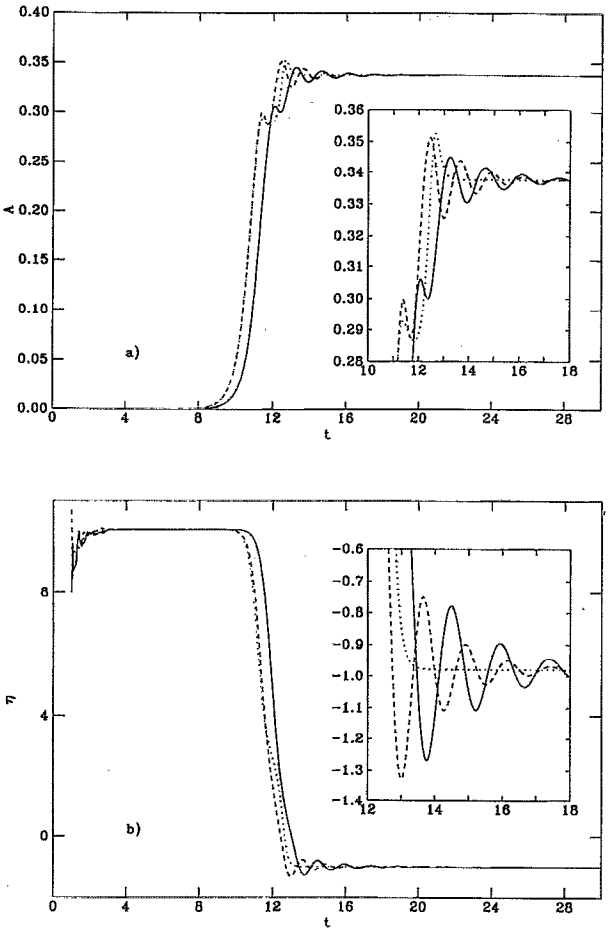

FIG. 4. As in Fig. 3 but for set II of parameters.

$\xi(t)$. The same sequence of random numbers is used in the numerical simulations of the original model and for the two approximations. The laser is assumed to be switched off for $t<0$ with $E=0$, and at $t=0$ the net gain parameter takes instantaneously a value $a>0$.

The numerical simulation of Eq. (1) indicates a rather long transient in which the steady state is not reached until many feedback delay times ($\tau=1$). The approach to the final state exhibits damped oscillations. For the first set of parameters (Fig. 3) the frequency evolves rather quickly to values close to its final one but the oscillations are long lived. For the second set of parameters (Fig. 4) the oscillations are more strongly damped but the main frequency jump does not occur until later than ten feedback delay times. In both cases there is a significant jump in the frequency during the transient. This jump occurs during the short time interval in which the time-dependent potential, Eq. (22), evolves from having a single minimum at $\eta\sim\theta a$ to its final form (see Figs. 1 and 2). We note that this jump is from the frequency associated with the off state of the laser rather than from the frequency of the laser in the absence of feedback, which is zero in our reference frame. The jump occurs when the growing amplitude exceeds a critical level. This is the random time at which the laser effectively switches on. It can be estimated by the time at which $A_0(t)$ acquires a value clearly above the noise level. This is the switch-on time in the absence of feedback whose mean value is known[16] to be $t\sim(1/2a)\ln\epsilon^{-1}$. This time gives an upper limit of the regime of exponential amplification of the initial fluctuations. At times earlier than $1/2a$ the dynamics is noise dominated and for times larger than the switch-on time nonlinear effects become important. Hence $V(\eta,t)$ gives a useful indication of the time of the frequency jump which can be identified as the time at which the potential reaches its asymptotic form found in Refs. 6 and 7.

In spite of the usefulness of $V(\eta,t)$, the generalization to the transient dynamics of the theory of Refs. 6 and 7 given by Eqs. (15) and (22) leads to an incorrect description of several gross qualitative features. In the first place, the approximation of the dynamics by an ordinary first-order differential equation is unable to describe the oscillatory approach to the final state. Second, and perhaps more important, is that solutions of this first-order equation lead in some switch-on events to a selection of a different final state from that chosen by the exact solution; this is easily identified by the error in the frequency. In Fig. 3(b) it is seen that while the exact solution leads to a frequency associated with the absolute minimum of $V(\eta,t)$, the approximate model using Eqs. (15) and (22) leaves the system hung up at a frequency associated with the local minimum to the right of the absolute minimum. This frequency is visited during the transient dynamics in both models but the system does not escape from it in the approximate solution. For the same set of parameters as used for Fig. 3(b) but with $\omega_0=0$ we have observed other events in which the solution of Eqs. (15) and (22) leads to a local minima of $V(\eta,t)$ much higher than the absolute minimum. The incorrect evolution of η also leads to an incorrect final value of the amplitude via Eq. (20) as seen in Fig. 3(a). The possibility of an incorrect final frequency obtained from Eqs. (15) and (22) disappears for set II of parameters in which $V(\eta,t)$ has a single minimum.

In contrast with the approximation based on the time-dependent potential $V(\eta,t)$ our simulations of Eq. (1) give good agreement for all times with the approximation in Eqs. (20) and (21). It always gives the correct selected frequency and displays the observed oscillatory approach to the final state. However, our improved approximation reaches the final state slightly faster than the exact solution: The final oscillations are more rapidly damped when these are long lived (set I) and the main frequency jump is advanced in time for set II.

In summary, we have a good approximation which reproduces individual switch-on events but a potential description of the dynamics of frequency selection is not possible. Still, the time-dependent potential, Eq. (20), is useful for identifying the time of main frequency jump and the selection of one of the possible final states.

IV. TRANSIENT INTENSITY AND FREQUENCY STATISTICS

In this section we analyze the transient statistics obtained from averages over 4000 independent switch-on events. Results from the simulation of Eq. (1) are com-

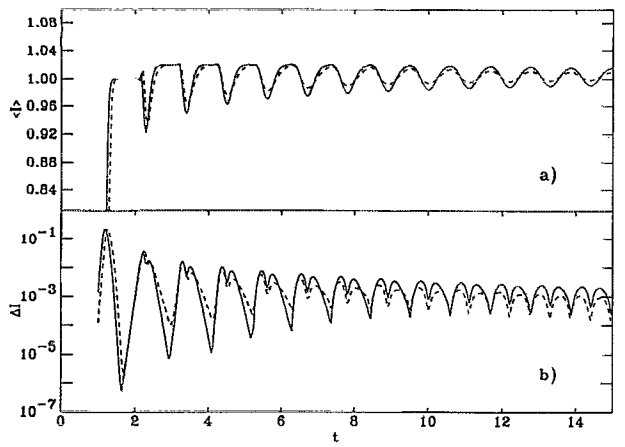

FIG. 5. (a) Average intensity and (b) standard derivation of intensity fluctuations for parameter set I, obtained from averages over 4000 realizations of Eq. (1) (solid line) and Eqs. (20) and (21) (dashed line). Note the logarithmic scale in (b).

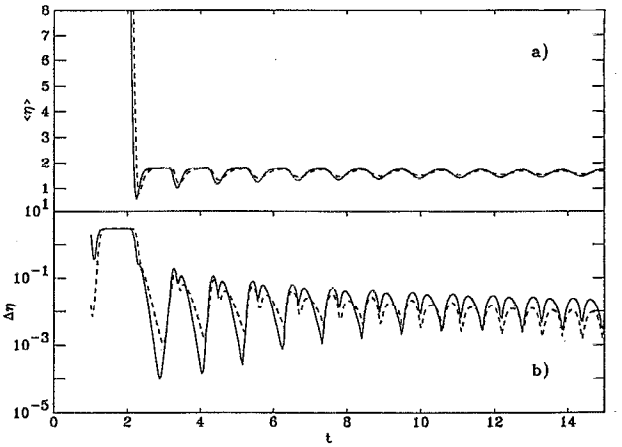

FIG. 6. The same as Fig. 5 for the average of (a) η and (b) the standard deviation of its fluctuations.

pared with those obtained from simulations of Eqs. (20) and (21) in Figs. 5–8. The agreement is rather good. The mean intensity $\langle I\rangle$, $I\equiv A^2$, shows the same oscillations about the final state that are seen in the individual switch-on events. The fact that the averaging does not kill these oscillations indicates that the switch-on time of the different events has a distribution with a standard deviation smaller than the period of oscillations. The small dip observed during the growth of the intensity for the second set of parameters in Fig. 4(a) leaves a trace in Fig. 7(a), but the average intensity has a monotonic growth. The standard deviation of the time-dependent intensity fluctuations, $\Delta I\equiv(\langle I^2\rangle-\langle I\rangle^2)^{1/2}$, shows oscillations with a first large peak during the growth of the mean intensity [Figs. 5(b) and 7(b)]. For each delay feedback time $\tau=1$ there is an oscillation of $\langle I\rangle$ and there are two peaks in ΔI. The peaks of ΔI are due to the shifting in time of the different individual events. In Fig. 7(b), ΔI has a minimum for $t\sim 12$ associated with the dip in the growth of the intensity for individual events for the second set of parameters.

The mean frequency evolves similarly to the frequency evolution in individual events. The standard deviation of the fluctuations in the mean frequency, $\Delta\eta\equiv(\langle\eta^2\rangle-\langle\eta\rangle^2)^{1/2}$, shown in Figs. 6 and 8 becomes very large at the time of the frequency jump. This indicates that in the dynamics of frequency selection a large range of values of the frequency can be observed in different switch-on events. This is a consequence of the randomness of the switch-on times. The maximum standard deviation of the frequency fluctuations is comparable with the frequency differences between closest solutions of Eq. (8). However, the subsequent peaks of $\Delta\eta$ during the oscillations are much smaller and they do not indicate jumps among the steady state of different possible frequencies. They are rather associated with fluctuations following an oscillatory behavior around the deepest minimum of $V(\eta,\infty)$. In summary, we conclude that the transient dynamics initially exhibit large frequency fluctuations but that the frequency associated with the minimum of $V(\eta,\infty)$ is selected with very high probability. This frequency corresponds to the solution with narrowest linewidth. Jumps among the solutions of Eq. (4) with different frequencies might occur by an activation mechanism on much longer time scales.

Measurements of temporal and spectral properties of switching transients such as studied here would demonstrte that feedback-induced oscillations are different from what is often called mode competition. In steady-state operation with noise, one expects both the AM and FM spectra to show peaks at other external cavity mode frequencies. In contrast, the modulations observed in the transient result from correlated AM and FM fluctuations which modulate the amplitude and frequency coherently in time.

V. STEADY-STATE SPECTRA

In this section, we consider the spectra of fluctuations in the steady-state regime. Spectra have been calculated for models of semiconductor lasers using field and carrier number equations such as the Lang–Kobayashi equations.[12] Calculated spectra[17–19] and experimental measurements[18,20,21] show strong evidence that the intensity power spectrum has additional peaks located at distances from the primary peak given approximately by the intermode spacing of the external cavity modes. The electric-field spectrum and the frequency spectrum have similar additional peaks at what are approximately the unexcited external cavity frequencies. Feedback reduces the linewidth of the field spectrum, as intended.

Previous studies that include the material dynamics for semiconductor or solid-state lasers have shown that these lasers are more susceptible to undamped pulsations when the feedback-induced oscillations match the relaxation oscillation frequency in some rational ratio. Clearly the oscillations induced by the transient might be used to suppress relaxation oscillations if the feedback oscillations were timed to be out of phase with the relaxation oscillations. The important key would be for the feedback to begin to suppress the rapidly growing intensity before it crossed the ultimate steady-state value. Our studies give an

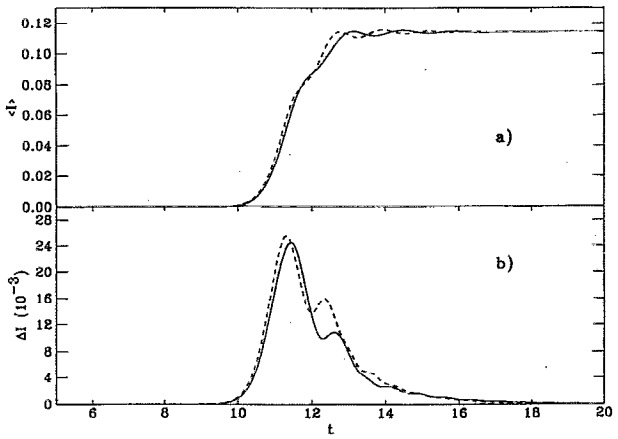

FIG. 7. (a) Average intensity and (b) standard deviation of intensity fluctuations for parameter set II, obtained from averages over 4000 realizations of Eq. (1) (solid line) and 2000 realizations of Eqs. (20) and (21) (dashed line).

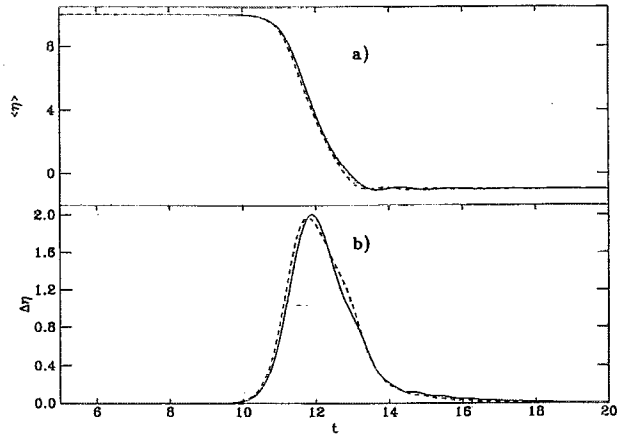

FIG. 8. The same as Fig. 7 for the average of (a) η and (b) the standard deviation of its fluctuations.

indication of the time scales involved and thus of the feedback delay times that would be required to accomplish this.

Of interest here is the degree to which the desired feedback-induced narrowing of the low-frequency portion of the spectrum of fluctuations around the final states is degraded in its usefulness by the excess power in other portions of the spectrum and the degree to which various approximate models give an adequate representation of this effect. Although our models for the evolution of the field will not have the relaxation oscillation resonance characteristic of the field-carrier number equations, we can still see the degree to which the further potential-based approximations neglect features of the noise spectrum that are induced purely by the feedback. For this purpose we could calculate the spectrum by using the results of others[18] who have calculated these spectra for models incorporating the field and carrier number dynamics and taking the limit of an infinite relaxation rate for the carrier number. Alternatively, we follow here the direct procedure of linearizing our Eqs. (3) and (4) around the deterministic steady solutions for the amplitude (modulus of the complex electric field) and phase. By this method we calculate the amplitude and frequency spectra which show sideband peaks associated with the external cavity modes due to the feedback. Later, we derive an expression [Eq. (42) below] relating the electric-field spectrum to that of the amplitude and phase, containing also a crossed term. In this way we investigate the effect of such peaks in the electric-field spectrum.

Writing

$$\varphi(t)\equiv\omega t+\delta(t), \tag{24}$$

where ω is one of the solutions of Eq. (8), and

$$A(t)\equiv A_D+u(t), \tag{25}$$

where A_D is the deterministic asymptotic value of the amplitude in Eq. (7), the linearization consists in neglecting terms of order $u(t)^2$, $[u(t)-u(t-\tau)]^2$, and $[\delta(t)-\delta(t-\tau)]^2$. No term in $\delta(t)^2$ appears. Solving the linearized equations for the Fourier transforms $\hat{\delta}(z)$ and $\hat{u}(z)$ of $\delta(t)$ and $u(t)$, respectively, we obtain

$$\langle|\hat{\delta}(z)|^2\rangle=\frac{2\epsilon}{|D|^2}\left(|c_1|^2+|c_2|^2/A_D^2\right), \tag{26}$$

$$\langle|\hat{u}(z)|^2\rangle=\frac{2\epsilon}{|D|^2}\left(|c_3|^2+|c_4|^2/A_D^2\right), \tag{27}$$

where

$$\begin{aligned}
&D\equiv c_1c_4-c_2c_3,\\
&c_1\equiv 2b\theta A_D-Q(1-e^{-iz\tau}),\\
&c_2\equiv 2bA_D^2+R(1-e^{-iz\tau})+iz,\\
&c_3\equiv iz+R(1-e^{-iz\tau}),\\
&c_4\equiv A_D^2Q(1-e^{-iz\tau}),\\
&R\equiv\gamma\cos[(\omega+\omega_0)\tau],\\
&Q\equiv\gamma\sin[(\omega+\omega_0)\tau]/A_D.
\end{aligned} \tag{28}$$

For comparison, the same linearization can be repeated for the different approximations discussed in the previous sections. In the stationary regime that we study here, our approximation in Eqs. (20) and (21) reduces to the simpler adiabatic approximation Eqs. (9) and (10). The resulting phase and amplitude spectra are

$$\langle|\hat{\delta}_A(z)|^2\rangle=\frac{2\epsilon}{A_D^2}\frac{1+\theta^2}{z^2-2zG\sin(z\tau)+2G^2[1-\cos(z\tau)]}, \tag{29}$$

and

$$\langle|\hat{u}_A(z)|^2\rangle=\frac{2\epsilon}{A_D^2}\left[|c_A|^2+|(2bA_D)^{-1}-c_A\theta|^2\right]. \tag{30}$$

We have introduced

$$G \equiv -\gamma\sqrt{1+\theta^2}\cos[(\omega+\omega_0)\tau+\arctan\theta], \tag{31}$$

$$F \equiv (-\gamma/2bA_D)\sin[(\omega+\omega_0)\tau], \tag{32}$$

and

$$c_A \equiv \frac{F(1-e^{-iz\tau})}{iz-G(1-e^{-iz\tau})}. \tag{33}$$

In the same way, our time-dependent potential, Eq. (22), reduces to Eq. (16) at late times. The linear phase spectrum can be calculated by linearizing Eq. (15) around the stationary solution, $\eta=\omega\tau$, and then using the relationship Eq. (13) between φ and η, which in Fourier space reads

$$\hat{\eta}(z) = (1-e^{-iz\tau})\hat{\varphi}(z). \tag{34}$$

The result is

$$\langle|\hat{\delta}_P(z)|^2\rangle = \frac{4\epsilon}{A_D^2}\frac{4+\theta^2}{[1-\cos(z\tau)][4(\tau^{-1}-G)^2+z^2]}. \tag{35}$$

The amplitude spectrum is again Eq. (30) but with c_A replaced by

$$c_P \equiv \frac{2F}{iz+2(\tau^{-1}-G)}. \tag{36}$$

The frequency spectrum $\hat{C}_{ff}(z)$ is

$$\hat{C}_{ff}(z) = z^2\langle|\hat{\delta}(z)|^2\rangle. \tag{37}$$

Figure 9 shows the amplitude and frequency spectra for fluctuations around the state corresponding to the deepest well ($\omega\approx 1.61$) in the potential of Fig. 1(b) and Fig. 10 shows these spectra for the adjacent and next deepest well ($\omega\approx -4.10$), both for parameter set I. Figure 11 shows these results for the only potential well ($\omega\approx -0.98$) of parameter set II. The amplitude spectra are normalized to obtain the relative intensity noise (RIN) spectra, which is the spectrum of fluctuations in the intensity divided by the mean (deterministic) value of the intensity squared. The relationship between the RIN spectrum and the amplitude spectrum is:

$$\mathrm{RIN} = 4\frac{\langle|\hat{a}(z)|^2\rangle}{A_D^2}. \tag{38}$$

From the figures, we see that for the RIN spectra, the potential approximation fails to reflect additional peaks in the spectrum while the adiabatic approximation qualitatively agrees more closely with the exact solution. The peaks in the exact solution are shifted a small amount closer to zero frequency than in our adiabatic approximation. Perhaps the only qualitative failure of the adiabatic approximation is that it overestimates the effect of the noise at high frequencies. This was expected from our discussion in Sec. II: The adiabatic approach should fail for frequencies higher than a, the typical time scale for relaxation of amplitude perturbations, since the amplitude cannot adiabatically follow such high frequencies.

The frequency spectra can be understood as follows: The strongest approximation in the potential approach is

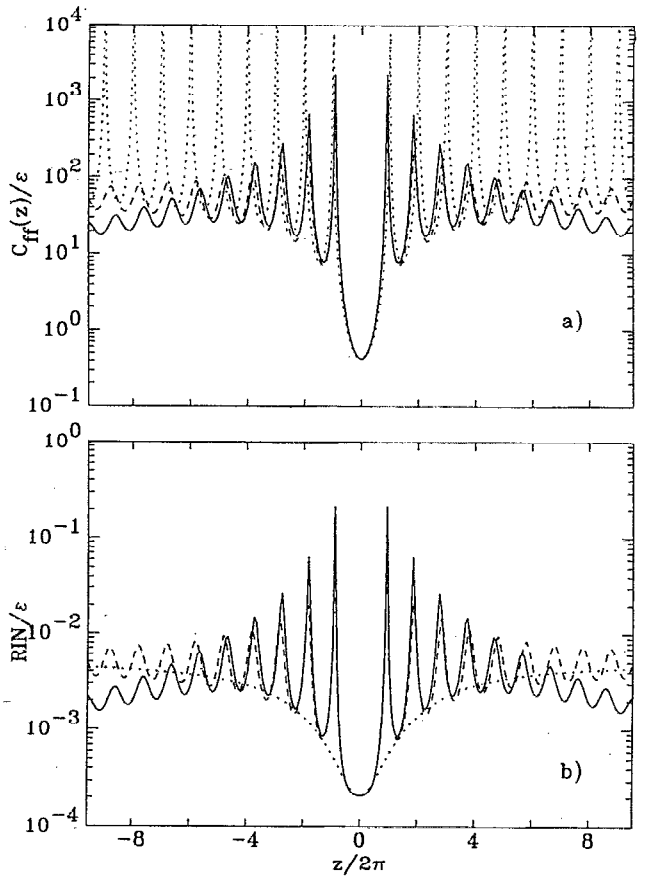

FIG. 9. (a) Frequency spectra and (b) relative intensity noise spectra for parameter set I, from linearization around the state with $\omega\approx 1.61$. Solid line is the result from the exact dynamics, dashed line from the adiabatic approximation, and dotted line from the potential approximation.

the replacement in Eq. (14) of a finite difference by derivatives. Since this is clearly incorrect for time scales shorter than τ, the spectra in the potential approximation should contain unphysical features at Fourier frequencies of order of higher than $2\pi/\tau$. This is what is seen in the frequency spectrum: The potential approximation presents divergencies at Fourier frequencies which are multiples of $2\pi/\tau$. They come from the trigonometric factor in the denominator of Eq. (35), which is a consequence of Eq. (34). Again, the adiabatic approximation does a better job of reflecting the spectrum of the exact solution, up to frequencies of order a. It is worth noting, however, that all the approximations reproduce the correct value for the frequency spectra at Fourier frequency $z=0$. Since this value is precisely the linewidth (full width at half-maximum) of the main Lorentzian contribution to the complex field spectrum,[5,21] we see that both approximations reproduce the exact value of this low-frequency linewidth Δ_L.

For reference we show in Fig. 12 the spectra with no feedback for parameter set I. They have been obtained simply by taking the limit $\gamma\to 0$ in expressions Eqs. (26)–(36). Our approximations are clearly inaccurate in this regime, but still the value at $z=0$ is correctly reproduced. The peaks that appear in the frequency spectra in the po-

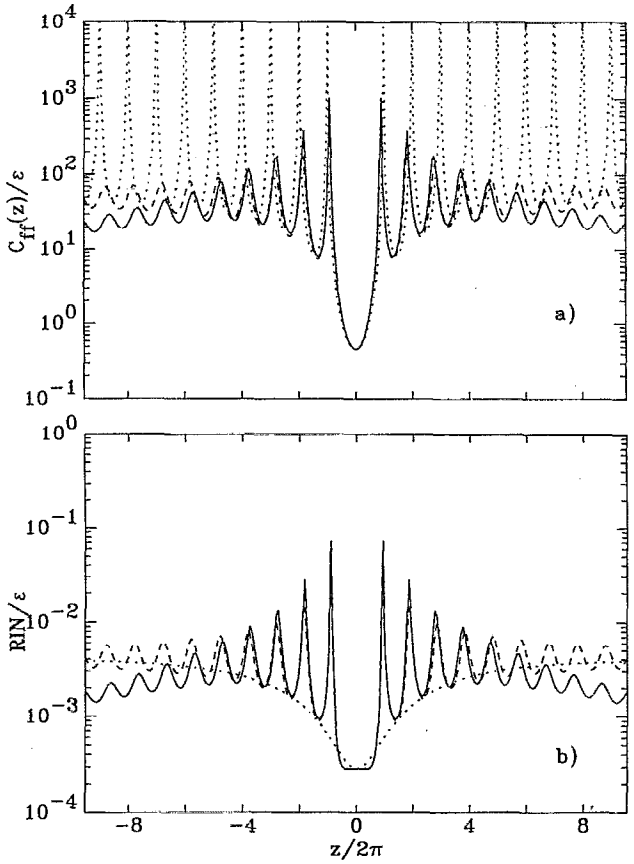

FIG. 10. Same as Fig. 9 but from linearization around the state with $\omega \approx -4.10$.

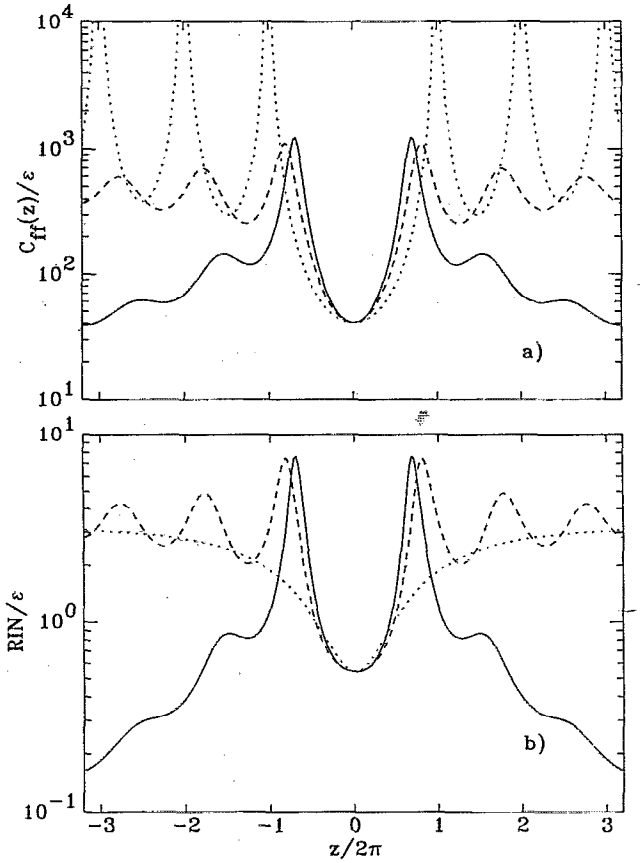

FIG. 11. (a) Frequency spectra and (b) relative intensity noise spectra for parameter set II, from linearization around the only possible steady state ($\omega \approx -0.98$). Meaning of the different lines is as in Fig. 9.

tential approximation at the external cavity resonance frequencies even with $\gamma=0$ indicate that there is an intrinsic error in this approximation in the relations governing behavior at frequencies of this magnitude or higher. Table I shows the linewidth reduction produced by the feedback for both sets of parameters. Two possible states for the first set of parameters are included. It is seen that the state corresponding to the deepest well in the potential is that of smaller linewidth. Note that Δ_L is always linear in ϵ, so that the tabulated values of Δ_L/ϵ are the same for any value of ϵ.

The sideband frequencies in the frequency and amplitude spectra also produce sideband peaks in the complex field spectrum, thus degrading the usefulness of the central linewidth reduction. An alternate definition of linewidth Δ_H, which contains information about higher frequencies, is given by[21]

$$\frac{1}{2}\int_{\Delta_H/2}^{\infty} dz \langle |\hat{\delta}(z)|^2 \rangle = 1. \tag{39}$$

When the complex field spectrum is a Lorentzian, $\Delta_L=\Delta_H$. It is clear that the definition of Eq. (39) cannot be applied to the potential approximation, because the divergencies at multiples of $2\pi/\tau$ will always give an infinite value to Δ_H. Calculation of Δ_H for the value $\epsilon=10^{-20}$ considered in this paper gives the same values as Δ_L in both the exact and in the adiabatic calculation. This shows that, for this value of the noise intensity, the complex field spectrum produced by Eq. (1) is essentially a Lorentzian of linewidth Δ_L, with sideband peaks of negligible weight. Then, both adiabatic and potential approximations correctly describe this linewidth, although in the potential case the second definition Δ_H cannot be applied.

To confirm this picture, we calculate the complex field spectrum as follows: First we write the complex electric field as

$$E(t)=[A_D+u(t)]e^{i\mu t}e^{i\delta(t)} \approx A_D\, e^{i\mu t+i\delta(t)+u(t)/A_D}, \tag{40}$$

where $\mu \equiv \omega+\omega_0$. In the last equality, use has been made of the assumed smallness of the fluctuations $u(t)$. Next, we construct the correlation function

$$C_{EE}(s) \equiv \langle E^*(t)E(t+s)\rangle - \langle E^*(t)\rangle\langle E(t+s)\rangle. \tag{41}$$

The averages are readily expressed in terms of phase and amplitude correlation functions by use of the Gaussian statistics implied by the smallness of fluctuations. The low-frequency singular behavior of the phase spectrum $[\langle |\hat{\delta}(z)|^2\rangle \to \Delta_L/z^2$ as $z\to 0]$ has to be taken explicitly into account and is responsible for the vanishing of $\langle E(t)\rangle$.

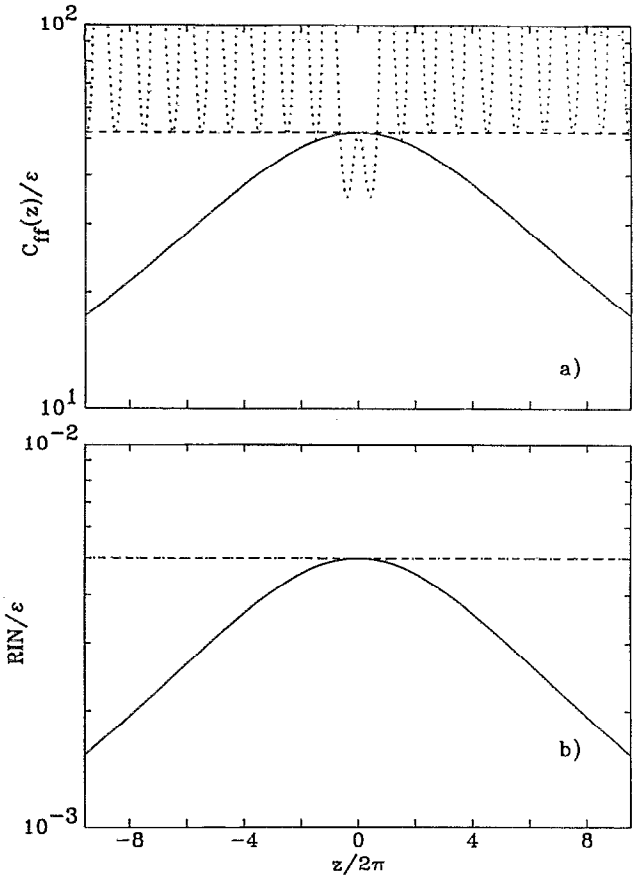

FIG. 12. (a) Frequency spectra and (b) relative intensity noise spectra for parameter set I but in the absence of feedback ($\gamma=0$). Meaning of the line is as in Fig. 9.

For small ϵ we find the following expression for the complex field spectrum, the Fourier transform of Eq. (41):

$$\frac{\hat{C}_{EE}(z+\mu)}{A_D^2}=\frac{\langle|\hat{E}(z+\mu)|^2}{A_D^2}$$

$$=(1-I_\delta+I_u)\frac{\Delta_L}{(\Delta_L/2)^2+z^2}$$

$$+\frac{1}{2\pi}\int_{-\infty}^{\infty}dt\frac{\Delta_L}{(\Delta_L/2)^2+(z-z')^2}$$

$$\times\left(\langle|\hat{\delta}(z')|^2\rangle-\frac{\Delta_L}{(z')^2}+\frac{\langle|\hat{u}(z')|^2\rangle}{A_D^2}\right.$$

TABLE I. Low-frequency linewidth Δ_L for different values of the parameters.

Parameter set	Δ_L/ϵ
Set I, $\gamma=0$	52.0
Set I, $\omega=1.61$	0.423
Set I, $\omega=-4.10$	0.460
Set II, $\gamma=0$	520
Set II	40.57

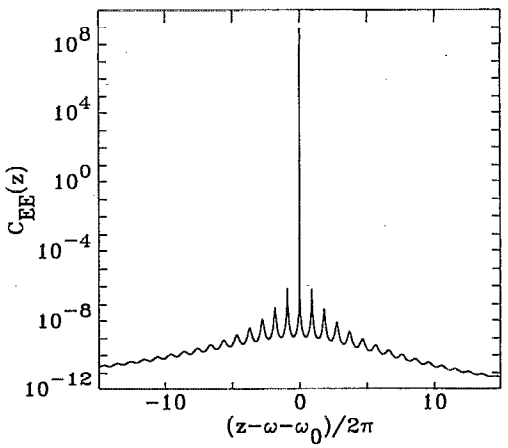

FIG. 13. Complex field spectrum for parameter set I, but with $\epsilon=10^{-8}$, from linearization of the exact dynamics.

$$+\frac{2}{A_D}\mathrm{Im}\langle\hat{u}(z')\hat{\delta}^*(z')\rangle\Bigg). \tag{42}$$

The last term in the integral, containing the imaginary part Im introduces asymmetry of the spectrum with respect to the central peak. We have defined

$$I_\delta\equiv\frac{1}{2\pi}\int_{-\infty}^{\infty}dz\left(\langle|\hat{\delta}(z)|^2\rangle-\frac{\Delta_L}{z^2}\right) \tag{43}$$

and

$$I_u\equiv\frac{1}{2\pi A_D^2}\int_{-\infty}^{\infty}dz\langle|\hat{u}(z)|^2\rangle. \tag{44}$$

This result confirms that the complex field spectrum is a Lorentzian of linewidth Δ_L with sidebands of order $\mathcal{O}(\epsilon^2)$ for small ϵ. We show in Fig. 13 a plot of Eq. (42) from the amplitude and phase spectra in Eqs. (26) and (27) for our set I of parameters, but with $\epsilon=10^{-8}$. This is a rather large value of the noise, but still realistic for some cases. The presence of sidebands reflecting the effect of the external cavity resonances is clear but their intensity is too small even for this value of noise to make an appreciable difference between Δ_L and Δ_H.

We present in Table II values of Δ_H for the sets of parameters discussed in this paper but with the value of ϵ arbitrarily raised to 10^{-2}, to show the effect of the sidebands. For set I, where a is not small, the adiabatic approximation again gives good results. It should be noted, however, that in the calculations of Table II (and in Fig. 13) we have still used the expressions for the phase spectra obtained by a linear calculation. We have not checked whether nonlinear corrections are important for these values of the noise intensity.

An important question is the impact of the sideband frequencies on the stability of the laser. It seems clear that the low-frequency portion of the spectrum and thus the basic laser linewidths would not be much disturbed. However, the frequency modulation that is evident in the frequency spectra indicates that the laser is changing its frequency in response to noise, including relatively long

TABLE II. High-frequency linewidth Δ_H from the exact equations and from the adiabatic approximation for several values of the parameters.

Parameter set ($\epsilon=10^{-2}$)	Δ_H/ϵ, exact	Δ_H/ϵ, adiabatic
Set I, $\gamma=0$	51.5	52.0
Set I, $\omega=1.61$	0.48	0.45
Set I, $\omega=-4.10$	0.50	0.49
Set II, $\gamma=0$	295.0	520.0
Set II	98.0	170.0

visitations to frequencies that are close to the center frequencies of the spectra from other coexisting states (other wells in the potential picture). This should significantly enhance the possibility of transitions to those other states (see, for example, the switchings described by Favre and co-workers in Ref. 20), though the transition processes clearly must involve nonlinear effects not taken into account in our spectral analyses.

VI. SUMMARY AND CONCLUSIONS

We have presented a variety of analyses of the transient processes of a laser with an external cavity, exploring approximations to the dynamics which are then compared to the exact solution. All of the approximations we explore are able to accurately present the low-frequency linewidth of the steady states. However, the more extreme approximations lead to errors in the transient selection of the steady-state solution, and to errors in the dynamical approach to the selected solution and to the spectrum of amplitude and frequency fluctuations about that solution. We have introduced a closed delayed equation for the phase of the electric field which captures most of these physical aspects of the system dynamics which are missed by the more severe approximations. Comparisons of transients, final state selection, and spectra are used to examine the limitations of each approximation. In particular, an adiabatically evolving potential for one-dimensional relaxational dynamics leads to an incorrect selected frequency. It appears that features of the exact spectra which are neglected in the more severe approximations may have a significant bearing on the stability of the various solutions and on their switching dynamics between different steady-state solutions.

ACKNOWLEDGMENTS

E.H.G. and M.S.M. acknowledge financial support from Comisión Interministerial de Ciencia y Tecnología (CICYT, Spain) Project TIC 90/080.

[1] N. Schunk and K. Petermann, IEEE J. Quantum Electron. **QE-24**, 1242 (1988).
[2] J. O. Binder and G. D. Cormack, IEEE J. Quantum Electron. **QE-25**, 2255 (1989).
[3] J. S. Cohen and D. S. Lenstra, IEEE J. Quantum Electron. **QE-25**, 1143 (1989).
[4] D. Lenstra and J. S. Cohen, SPIE Proc. **1376**, 245 (1991); H. Li, J. D. Park, L. Diego Marin, J. G. McInerney, and H. R. Telle, SPIE **1376**, 172 (1991).
[5] K. Petermann, *Laser Diode Modulation and Noise* (Kluwer, Dordrecht, 1988).
[6] J. Mørk and B. Tromborg, IEEE Photonics Lett. **PL-2**, 21 (1990); J. Mørk, M. Semkov, and B. Tromborg, Electron. Lett. **26**, 609 (1990).
[7] D. Lenstra, Opt. Commun. **81**, 209 (1991).
[8] N. A. Olsson and W. T. Tsang, IEEE J. Quantum Electron. **QE-19**, 1479 (1983).
[9] C. Etrich, A. W. McCord, and P. Mandel, IEEE J. Quantum Electron. **QE-27**, 937 (1991).
[10] R. Müller and P. Glas, J. Opt. Soc. Am. B **2** (1985); K. Vahala and A. Yariv, IEEE J. Quantum Electron. **QE-19**, 1096 (1983); G. Bjoerk and O. Nilsson, *ibid.* **QE-23**, 1303 (1987); K. Kikuchi and T. Okoshi, Electron. Lett. **18**, 10 (1982); O. Hirota and Y. Suematsu, IEEE J. Quantum Electron. **QE-15**, 142 (1979); T. Kanada and K. Nawata, **QE-15**, 559 (1979).
[11] T. Okoshi and K. Kikuchi, *Coherent Optical Fiber Communications* (Kluwer, Dordrecht, 1988), p. 114.
[12] R. Lang and K. Kobayashi, IEEE J. Quantum Electron. **QE-16**, 347 (1980).
[13] T. Mukai and K. Otsuka, Phys. Rev. Lett. **55**, 1711 (1985); K. Otsuka and H. Kawaguchi, Phys. Rev. A **30**, 1575 (1984); H. Kawaguchi and K. Otsuka, Appl. Phys. Lett. **45**, 934 (1984); R. Müller and P. Glas, J. Opt. Soc. Am. B **2**, 184 (1985); P. Glas, R. Müller, and A. Klehr, Opt. Commun. **47**, 297 (1983); P. Glas, R. Müller, and G. Wallis, *ibid.* **68**, 133 (1988); J. Sanchez, W. Elasaesser, and E. O. Goebel, Phys. Rev. Lett. **63**, 224 (1989); J. D. Park, D. S. Seo, J. G. McInerney, G. C. Dente, and M. Osinski, Opt. Lett. **14**, 1054 (1989); J. Mørk, J. Mark, and B. Tromborg, Phys. Rev. Lett. **65**, 1999 (1990); B. Tromborg and J. Mørk, IEEE Photonics Technology Lett. **PTL-2**, 549 (1990); IEEE J. Quantum Electron. **QE-26**, 642 (1990); J. Mørk, B. Tromborg, and J. Mark (unpublished).
[14] R. W. Tkach and A. R. Chiraplyvy, IEEE J. Lightwave Tech. **LT-4**, 1655 (1986).
[15] F. de Pasquale and P. Tombesi, Phys. Lett. A **72**, 7 (1979); F de Pasquale, P. Tartaglia, and P. Tombesi, Physica A **99**, 581 (1979); Z. Phys. B **43**, 353 (1981); Phys. Rev. A **25**, 466 (1982).
[16] M. San Miguel, SPIE Proc. **1376**, 272 (1991).
[17] H. Olesen, J. H. Osmundsen, and B. Tromborg, IEEE J. Quantum Electron. **QE-22**, 762 (1986).
[18] S. Spano, S. Piazolla, and M. Tamburrini, IEEE J. Quantum Electron. **QE-20**, 350 (1984).
[19] G. P. Agrawal, IEEE J. Quantum Electron. **QE-20**, 468 (1984).
[20] L. Goldberg, H. F. Taylor, A. Dandridge, J. W. Weller, and R. O. Miles, IEEE J. Quantum Electron. **QE-18**, 555 (1982); F. Favre, D. Le Guen, and J. C. Simon, *ibid.* **QE-18**, 1712 (1982); F. Favre and A. Le Guen, *ibid.* **QE-21**, 1937 (1985); H. Temkin, N. A. Olsson, J. H. Abeles, R. A. Logan, and M. B. Panish, *ibid.* **QE-22**, 286 (1986).
[21] Ph. Laurent, A. Clarion, and Ch. Breant, IEEE J. Quantum Electron. **QE-25**, 1131 (1989).